NANO LETTERS

2008
Vol. 8, No. 4
1192-1196

One-Step Nanoscale Assembly of Complex Structures via Harnessing of an Elastic Instability

Ying Zhang,[†,‡] Elisabetta A. Matsumoto,[†,§] Anna Peter,[†,‡] Pei-Chun Lin,[†,‡,||] Randall D. Kamien,[*,†,§], and Shu Yang[*,†,‡]

Laboratory for Research on the Structure of Matter, University of Pennsylvania, 3231 Walnut Street, Philadelphia, Pennsylvania 19104, Department of Materials Science and Engineering, University of Pennsylvania, 3231 Walnut Street, Philadelphia, Pennsylvania 19104, and Department of Physics and Astronomy, University of Pennsylvania, 209 South 33rd Street, Philadelphia, Pennsylvania 19104

Received January 16, 2008; Revised Manuscript Received February 18, 2008

ABSTRACT

We report on a simple yet robust method to produce orientationally modulated two-dimensional patterns with sub-100 nm features over cm^2 regions via a solvent-induced swelling instability of an elastomeric film with micrometer-scale perforations. The dramatic reduction of feature size (~10 times) is achieved in a single step, and the process is reversible and repeatable without the requirement of delicate surface preparation or chemistry. By suspending ferrous and other functional nanoparticles in the solvent, we have faithfully printed the emergent patterns onto flat and curved substrates. We model this elastic instability in terms of elastically interacting "dislocation dipoles" and find complete agreement between the theoretical ground-state and the observed pattern. Our understanding allows us to manipulate the structural details of the membrane to tailor the elastic distortions and generate a variety of nanostructures.

The demand for higher density, faster speed, and lighter devices drives the need for developing inexpensive fabrication tools that create ever more complex patterns with smaller features.[1] Many current fabrication techniques rely upon top-down processes;[2] Nature, on the other hand, provides us with examples of intrinsic, bottom-up effects from the phyllotactic growth of plants, to animal stripes, and to fingerprints. In those systems, instabilities, packing constraints, and simple geometries drive the formation of delicate, detailed, and beautiful patterns. Mechanical instabilities in soft materials, precipitated by dewetting, swelling, and buckling, are often viewed as failure mechanisms that can interfere with the performance of devices. Recently these instabilities have been exploited to assemble complex patterns,[2–10] to fabricate novel devices such as stretchable electronics[11] and microlens arrays,[12–14] and to provide a metrology for measuring elastic moduli and the thickness of ultrathin films.[15,16]

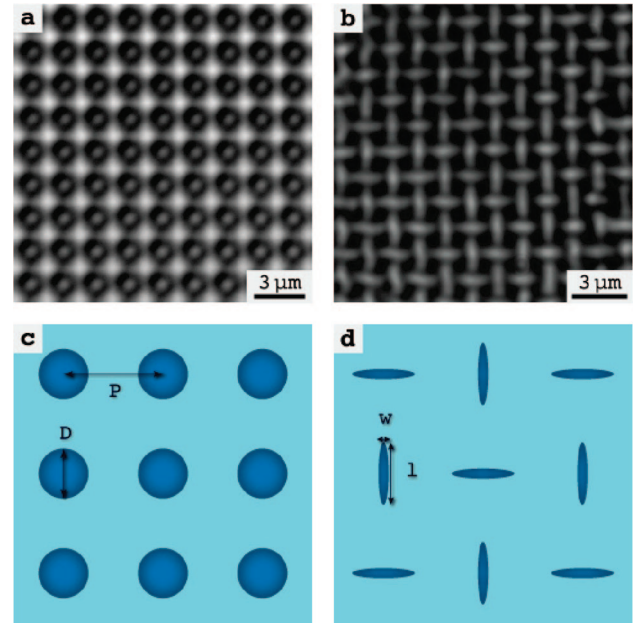

Figure 1. PDMS membrane with a square lattice of holes before and after swelling by toluene. Optical images of (a) the original PDMS membrane with hole diameter $D = 1$ μm, pitch $P = 2$ μm, and depth $H = 9$ μm, and (b) the swollen PDMS membrane with diamond plate structures. (c−d) Schematic illustration of (a) and (b), respectively.

* To whom correspondence should be addressed. E-mail: shuyang@seas.upenn.edu (S.Y.); kamien@physics.upenn.edu (R.D.K.).
† Laboratory for Research on the Structure of Matter, University of Pennsylvania.
‡ Department of Materials Science and Engineering, University of Pennsylvania.
§ Department of Physics and Astronomy, University of Pennsylvania.
|| Present address: Department of Mechanical Engineering, National Taiwan University, No. 1, Sec. 4, Roosevelt Road, Taipei, 10617, Taiwan.

10.1021/nl0801531 CCC: $40.75
Published on Web 03/12/2008

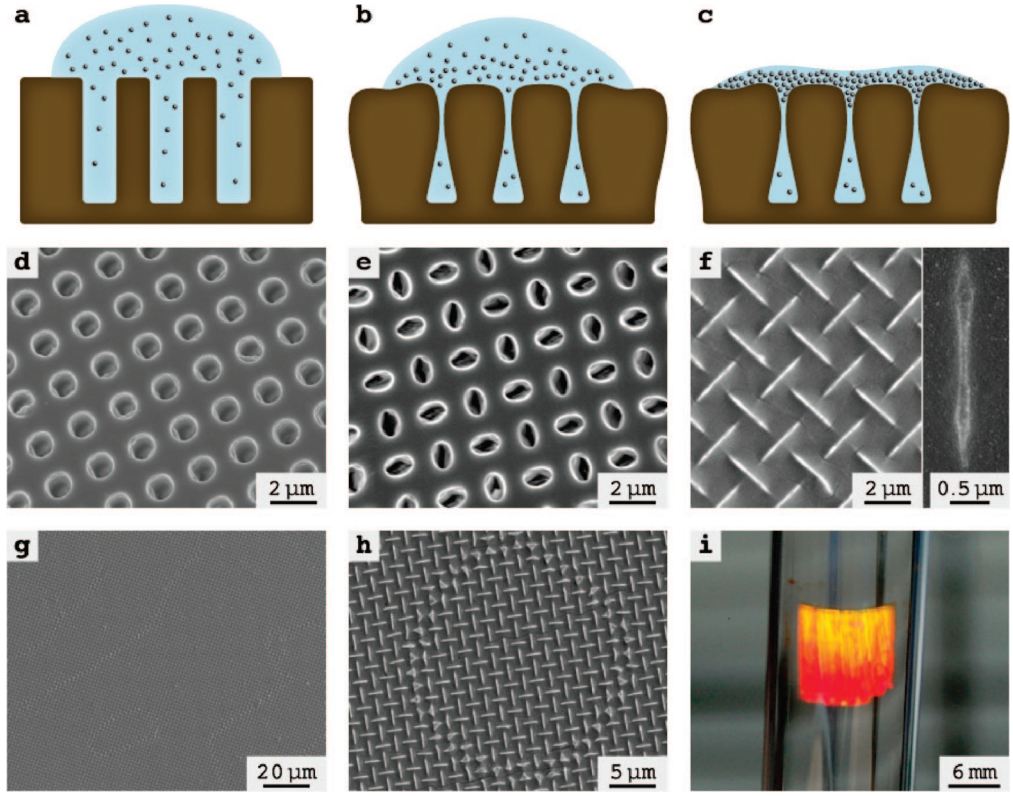

Figure 2. Convective assembly of Fe_3O_4 nanoparticles in toluene on the PDMS membrane with a square lattice of holes ($D = 1$ μm, $P = 2$ μm, and $H = 9$ μm). (a−c) Schematic illustration of the self-assembly process. (a) A solution of nanoparticles suspended in an organic solvent (e.g., toluene) is deposited onto the patterned PDMS membrane. (b) The organic solvent swells the PDMS membrane and deforms the holes into the diamond plate structure. (c) Nanoparticles convectively assemble on the swollen PDMS membrane, capturing the deformed structure. The nanoparticle film is then transferred to a glass substrate by microcontact printing. (d) Scanning electron micrograph (SEM) of the original PDMS membrane. (e) SEM of the deformed PDMS membrane after casting a drop of nanoparticle/toluene solution on PDMS, followed by heating in an oven at 65 °C for 2 h and removal of the nanoparticle film. The diamond plate structure can be clearly seen in the PDMS membrane although the shape is somewhat relaxed compared to that of nanoparticle assembly due to the elastic nature of the PDMS. (f) SEM of the nanoparticle pattern lifted off from the deformed PDMS membrane. Inset: higher magnification of an individual elliptical nanoparticle deposit, which is 78 nm wide by 2.3 μm long. The ridge height is 392 nm according to atomic force microscopy (AFM) section analysis. (g) A larger field of view of the nanoparticle pattern, illustrating high uniformity over a large area. (h) SEM of the dislocation in the diamond plate pattern. Note that the overall symmetry of the sample is unaffected by the defect. (i) Optical photography of the nanoparticle film that was transfer-printed on a glass capillary. The colorful reflection is due to the diffraction grating of the underlying pattern, which is determined by the periodicity and refractive index of the film and the viewing angle.

Along these lines, we have harnessed an elastic instability in a flexible poly(dimethylsiloxane) (PDMS) membrane with a periodic arrangement of circular pores. When exposed to a solvent, these pores elliptically deform and elastic interactions between them generate long-range orientational order of their axes into a "diamond plate" pattern. We lace the solvent with nanoparticles and find that solvent diffusion and evaporation drive the convective assembly[17–19] of the nanoparticles onto the PDMS surface along these distorted pores. The resulting uniform film can be transferred onto a glass substrate via contact printing. The features of the printed nanoparticle pattern are up to 10 times sharper than those of the original membrane. The membrane can be reused, and thus our method of nanoprinting through elastic patterning and convective assembly offers a one-step, repeatable process without the requirement of delicate surface preparation or chemistry. The resulting structural anisotropy of the nanoparticle films could be used to generate similar anisotropic magnetic, photonic, phononic, and plasmonic properties. Our technique could be implemented in other material systems such as polymers and composites that undergo swelling and brings a new design mechanism for device engineering.

PDMS is an elastomer that has been widely used in soft lithography for low-cost fabrication of microdevices.[20] Here, we have replica-molded a PDMS membrane with circular pores from an array of 1 μm diameter silicon pillars spaced 2 μm apart on a square lattice.[21] When exposed to an organic solvent, such as toluene, PDMS gels swell by as much as 130%.[22] As the osmotic pressure builds, the circular pores in the PDMS deform and eventually snap shut to relieve the stress (Figure 1a−d), much as the joints in railways and bridges expand and contract to maintain structural integrity in response to changes in moisture and temperature. The resulting "diamond plate" pattern persists over large regions of the sample. Because the elastic deformation of the PDMS membrane is induced by solvent swelling, the diamond plate pattern in PDMS is stable in the wet state and snaps back to the original square lattice once the solvent evaporates (see Figure S1 and the movie in the Supporting Information). To capture the diamond plate before evaporation and, more

importantly, to utilize this deformation for assembly of complex functional structures, we suspended superparamagnetic Fe_3O_4 nanoparticles (~10 nm in diameter) in toluene and applied the solution to the PDMS membrane (Figure 2a). As the PDMS swells (Figure 2b), the convective assembly of the nanoparticles follows (Figure 2c), which faithfully replicates the deformed PDMS membrane (Figure 2e−f). Once dried, the elastic membrane returns to its original state (Figure 2d) and can be reused. We find that the nanoparticle film can be transfer-printed onto another substrate, which can be either hydrophobic (e.g., Au and polystyrene) or hydrophilic (e.g., glass).[23,24] The ability to release our nanoparticle films from PDMS (i.e., the carrier) onto a targeted substrate may be attributed to the difference in particle−substrate adhesion,[25,26] which strongly depends on both the interfacial energy and contact area. During solvent evaporation, capillary forces hold the particles tightly together on the PDMS surface; the low surface energy and compliance of PDMS, on the other hand, maximizes the contact of nanoparticles on the hard substrate for subsequent transfer. Supporting this, we find that when air-dried for 2 h or dried in an oven at 65 °C for 10 min, the nanoparticle films could no longer be transferred effectively onto a hydrophilic substrate[23] and showed reduced film quality when transferred onto a hydrophobic surface. This observation suggests that residual solvent may play an important role in wetting, which increases the contact between the nanoparticle film and the target substrate, therefore increasing the adhesion and transfer yield.[26]

Scanning electron microscopy (SEM) (see Figure 2f inset) reveals a dramatic reduction in feature size: the width of each elliptic nanoparticle deposit (78 nm) is smaller than $^1/_{10}$ the diameter of the initial pore (1 μm). The separation between neighboring ellipses remains 2 μm, demonstrating that the deformation preserves the original lattice. Other groups[27] report similar feature size reduction, from ~1.6 μm to ~200 nm, however this comes about via several cycles of compression and replication of the PDMS molds.

Previously, the elastic instabilities of a polymer matrix have been harnessed to produce patterns exhibiting long-range order; when a polymer gel network is swollen by a solvent, the osmotic pressure competes with the elasticity of the inner gel surface to produce beautiful and regular wrinkle patterns with wavelengths on the order of tens to hundreds of micrometers.[3,7,16] Our approach differs in that we need not balance elastic forces with kinetic effects. Even more fascinating, our nanopatterning method does not require delicate template preparation or surface chemistry[28,29] and we achieve a ground state with long-range order. As shown in Figure 2g, this "diamond-plate" pattern persists over the entire sample (up to cm^2 in our experiments depending on the available size of the original Si master) with no random defects; the "phase slip" dislocations (Figure 2h) do not alter the overall symmetry of the system, thus preserving many of the interesting physical properties of the film. For instance, the brilliant red-orange image shown in Figure 2i is diffraction from our highly regular, optically anisotropic product.

To understand the response of the membrane under swelling, we have used continuum elasticity theory to model

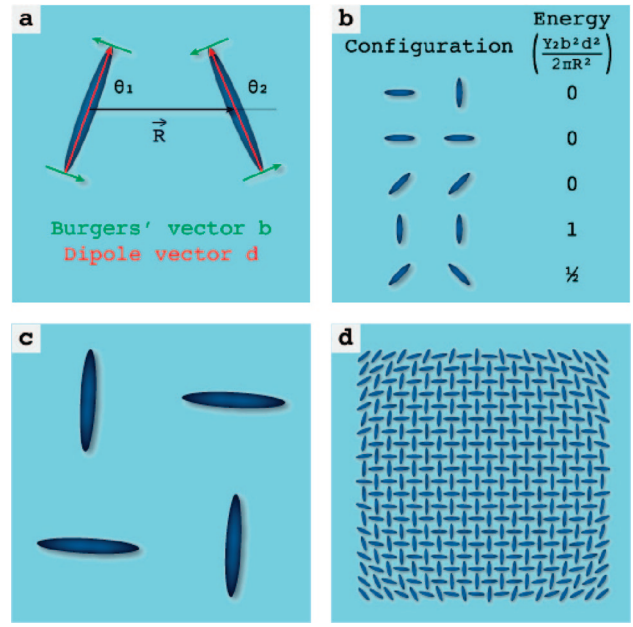

Figure 3. Theoretical calculation of minimum energy states of square lattice of holes using dislocation dipoles. (a) Diagram of the interaction between two dislocation dipoles separated by $\vec{R}$. The Burgers vector's density for a dislocation dipole of strength d located at $\vec{x}$ is $\vec{b}(\vec{x}) = \hat{z} \times \hat{d}\, b[\delta^2(\vec{x} - \vec{d}/2) - \delta^2(\vec{x} + \vec{d}/2)]$. (b) Several local configurations of pairs of dipoles and their respective energies per hole (offset by an angle-independent constant), all given in units $(Y_2b^2d^2)/2\pi R^2$. (c) The minimal energy configuration for a 2 × 2 plaquette of dipoles. The angles

$$\begin{bmatrix} \theta_1 & \theta_2 \\ \theta_3 & \theta_4 \end{bmatrix}$$

are $\theta_2 = \theta_3 = -^1/_2 \arcsin(^1/_{10}) \approx 0.05$, $\theta_1 = \theta_4 = \theta_2 + \pi/2$. This configuration has an energy of $-2.55(Y_2b^2d^2)/(2\pi R^2)$. (d) Minimum energy configurations 20 × 20 square lattice of holes obtained by numeric minimization of the pairwise interactions of a 20 × 20 square lattice of dipoles.

the local deformation of each pore as a small amount of material inserted into an unstressed elastic sheet. Formally, we may view this insertion as two equal and opposite edge dislocations with macroscopic Burgers vectors forming an effective "dislocation dipole" (as defined in Figure 3a). According to linear elasticity theory,[30] the energy of a deformation given in terms of the linearized strain tensor $u_{ij} = (\partial_i u_j + \partial_j u_i)/2$ is

$$E = \frac{1}{2}\int d^2x[\lambda(u_{ii})^2 + 2\mu(u_{ij})^2] \qquad (1)$$

where λ and μ are Lamé coefficients. However, to find the ground-state configuration, we need only consider the energy of interaction between two dislocation elements, as the self-energy is independent of the orientation of the dislocation dipole. The interaction energy per hole of two dislocation dipoles is dependent only on their dislocation densities $\vec{b}_1(\vec{x})$ and $\vec{b}_2(\vec{x})$

$$E = \frac{Y_2}{2}\int \frac{d^2q}{(2\pi)^2}\frac{(\vec{q}\times\vec{b}_1(\vec{q}))\cdot(\vec{q}\times\vec{b}_2(-\vec{q}))}{q^4} \qquad (2)$$

where $Y_2 = 4\mu(\lambda + \mu)/(\lambda + 2\mu)$ is the two-dimensional Young's modulus. From this expression, we obtain the interaction energy per hole

$$E = -\frac{Y_2}{2\pi}\frac{b_1 d_1 b_2 d_2}{R^2}\left[\cos(\theta_1+\theta_2)\sin(\theta_1)\sin(\theta_2)+\frac{1}{4}\right] \quad (3)$$

where θ_1 and θ_2 are the angles each dipole makes with respect to the vector separating them and R is the distance between them (see Figure 3a). The long-range behavior of the interaction is responsible for the long-range order. The energies of several local configurations are shown in Figure 3b. The ground-state configuration for a given lattice is determined by minimizing the sum of all possible pairwise interactions over each angle. The ground state of a 2 × 2 plaquette of holes is a set of mutually perpendicular dislocation dipoles (Figure 3c). Numeric minimization of the energy for larger square lattices (Figure 3d) corroborates not only the results of the 2 × 2 plaquette (Figure 3c) but also those of our experiments (Figure 1b). Moreover, we see that the larger lattices have a higher degree of alignment with the lattice axes, confirming that interaction with distant dipoles is essential and provides the long-range fidelity of the patterns over centimeter length scales. Our model should apply at all length scales: indeed, the resulting diamond plate aligned along the two lattice directions is similar to the deformation pattern recently seen in 10 × 10 arrays of millimeter size holes in elastomeric cellular solids subjected to uniaxial compression.[31]

Because the emergent pattern is the result of energy minimization of the neighboring pores upon deformation, we can tune the specific characteristics of each nanoparticle film simply by changing the diameter and spacing of the holes and the lattice symmetry in the PDMS membrane. Figure S2 (Supporting Information) shows diamond plates with different lengths and widths obtained from the square lattice of the PDMS membranes with variable pore size and spacing, demonstrating the transferability of our simple process. The dipole interactions require that the swollen regions around each pore overlap. Thus, the spacing of the pores and the rate of diffusion can influence the diamond plate pattern. In our experiments the diamond plate is obtained in PDMS membranes with high aspect ratios (height H/diameter D = 2 to 18) and pitch P/diameter D ratios up to 6.

The analytic model posed here enables us to rationally design new motifs via externally imposed elastic forces. By mechanically stretching the perforated PDMS membrane with square lattice along a lattice direction (Figure 4a),[32] we exert an external force on the dislocation dipoles favoring alignment along the strain direction. This competes with the internal stresses caused by swelling, and by varying the strength of the external stress, we are able to create an even richer library of morphologies. These patterns vary continuously from slight distortions of the original pattern up to 10% strains, to a binary pattern of circles and lines from 30–50% strain, to a rectangular lattice of aligned ovals for strains in excess of 50% (see Figure 4b−c).

We have demonstrated a one-step method for the rational design of functional nanoscale motifs with adjustable feature size and shape. By taking advantage of the elastic instability

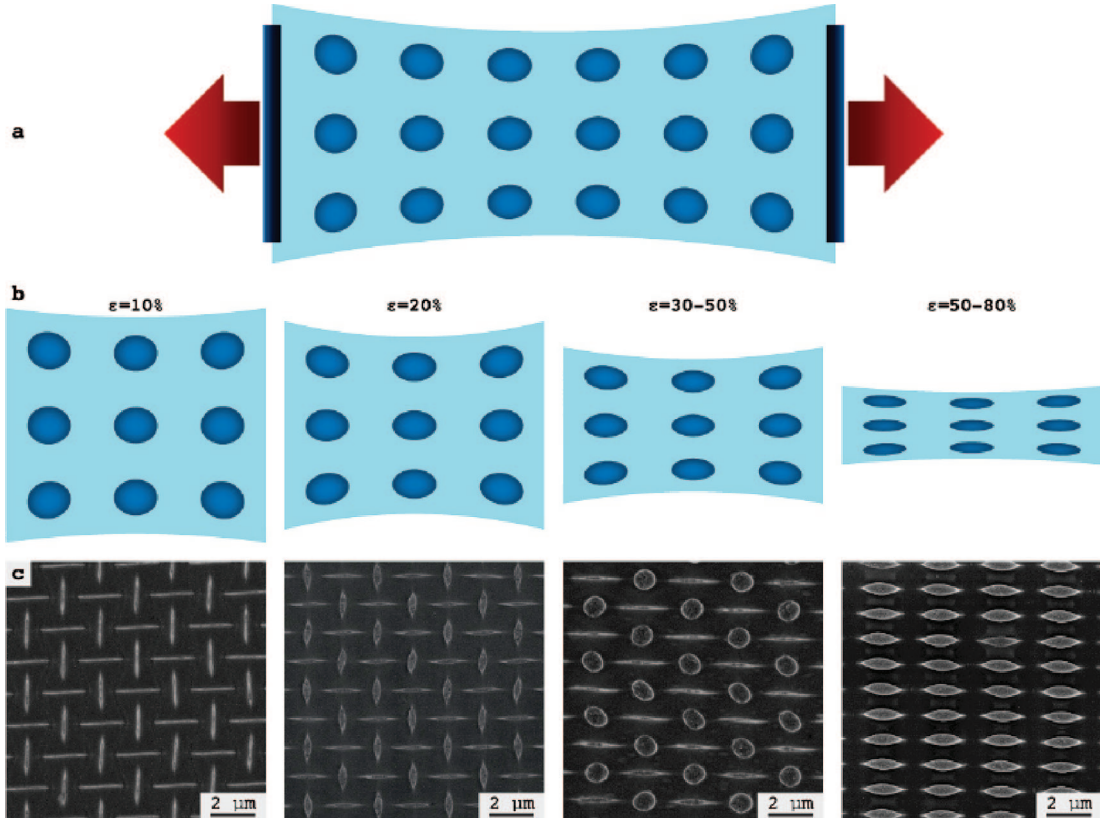

Figure 4. Complex patterns of Fe_3O_4 nanoparticle assembly obtained from PDMS membranes that are mechanically stretched at different strain levels. (a) Schematic illustration of the mechanical stretching of the PDMS membrane. (b) Schematics of the lattice configurations at different strain levels. (c) Corresponding SEM images of Fe_3O_4 nanoparticle assemblies from the stretched PDMS membranes. The original membrane has a square lattice of holes with D = 750 nm, P = 1.5 μm, and H = 9 μm.

caused by swelling in a patterned elastomeric membrane, we offer an elegant means to direct the formation of complex ordered patterns while simultaneously capturing nanoparticles into structured films via convective assembly. Simply changing parameters in the patterned PDMS membrane facilitates transformation to complex morphologies. These structures are easily transferred to both flat and curved surfaces as well as superimposed to create multilayered devices. We anticipate that the method presented here will be the basis for designing new tools in nanoscale manufacturing and for dynamically tunable structures.

Experimental Section. Replica-Molding of Patterned PDMS Membrane.[21]Silicon masters with a square lattice of cylindrical pillars were fabricated by the conventional 248 nm photolithography/etching process. The pillars have diameter D ranging from 350 nm to 2 μm, pitch P ranging from 800 nm to 5 μm, and height H ranging from 4 to 9 μm, respectively. The silicon masters were cleaned by sonication in deionized water, isopropyl alcohol, and acetone for 10 min, respectively. They were then placed in the oxygen plasma cleaner (PDC-001, Harrick Scientific Products, Inc.) at 23 W for 10 min. Finally, they were silanized with release agent (tridecafluoro-1,1,2,2-tetrahydrooctyl)trichlorosilane vapor (Gelest Inc.) for 2 h under vacuum in a desiccator. The PDMS prepolymer and its curing agent (RTV615, GE Silicones) were mixed in a weight ratio of 10:1 and degassed to remove air bubbles. The prepolymer mixture was poured onto the silicon master and cured in a convection oven at 80 °C for two hours before removal by careful pealing.

Convective Assembly of Fe_3O_4 Nanoparticles on PDMS Membrane. Superparamagnetic Fe_3O_4 nanoparticles (average diameter of 10 nm) were extracted from a commercially available ferrofluid (EMG911, Ferrotec Corporation, USA). First, 5 mL of acetone was added into 1 mL of ferrofluid to precipitate the nanoparticles, which were then collected using a strong magnetic bar. The nanoparticles were washed with acetone three times and redispersed into toluene with a concentration of 2.5% w/v. A small amount of the Fe_3O_4 nanoparticle toluene solution was applied onto the PDMS membrane using a cotton swab and blow-dried under N_2 for 20 s. The obtained thin nanoparticle film was then transfer-printed onto a cover glass and lifted off from the PDMS membrane for further study.

Convective Assembly of Fe_3O_4 Nanoparticles on Mechanically Stretched PDMS Membranes. A customized jig was constructed from a large acrylic base and two sliders whose positions could be adjusted continuously by two long-thread M4 wing screws. Small binder clips connected to each of the two sliders were clamped to the edges of the PDMS membrane (see Figure 4a). After stretching the PDMS membrane,[32] the nanoparticle solution was applied using the same method described above.

Acknowledgment. We thank J. Ashley Taylor (University of Wisconsin) for providing some Si masters and Dinesh Chandra for insightful discussion. This work was supported by NSF MRSEC DMR05-20020. Y.Z., P.L., and S.Y. were also supported in part by NSF CAREER award DMR-0548070 and a 3M Nontenured Faculty Grant. E.M. and R.D.K. were supported in part by gifts from L. J. Bernstein and H. H. Coburn.

Supporting Information Available: In-situ optical and AFM images of partially restored perforated PDMS membrane during toluene evaporation shown in Figure 1 and corresponding video (.qt). SEM images of Fe_3O_4 nanoparticle assemblies from different PDMS membranes with square lattices. This material is available free of charge via the Internet at http://pubs.acs.org.

References

(1) Miller, R. D. *Science* **1999**, *286*, 421.
(2) Geissler, M.; Xia, Y. N. *Adv. Mater.* **2004**, *16*, 1249.
(3) Tanaka, T.; Sun, S. T.; Hirokawa, Y.; Katayama, S.; Kucera, J.; Hirose, Y.; Amiya, T. *Nature* **1987**, *325*, 796.
(4) Bowden, N.; Brittain, S.; Evans, A. G.; Hutchinson, J. W.; Whitesides, G. M. *Nature* **1998**, *393*, 146.
(5) Herminghaus, S.; Jacobs, K.; Mecke, K.; Bischof, J.; Fery, A.; Ibn-Elhaj, M.; Schlagowski, S. *Science* **1998**, *282*, 916.
(6) Genzer, J.; Groenewold, J. *Soft Matter* **2006**, *2*, 310.
(7) Klein, Y.; Efrati, E.; Sharon, E. *Science* **2007**, *315*, 1116.
(8) Grzybowski, B. A.; Bishop, K. J. M.; Campbell, C. J.; Fialkowski, M.; Smoukov, S. K. *Soft Matter* **2005**, *1*, 114.
(9) Hendricks, T. R.; Lee, I. *Nano Lett.* **2007**, *7*, 372.
(10) Jiang, C.; Singamaneni, S.; Merrick, E.; Tsukruk, V. V. *Nano Lett.* **2006**, *6*, 2254.
(11) Khang, D. Y.; Jiang, H. Q.; Huang, Y.; Rogers, J. A. *Science* **2006**, *311*, 208.
(12) Chan, E. P.; Crosby, A. J. *Adv. Mater.* **2006**, *18*, 3238.
(13) Holmes, D. P.; Crosby, A. J. *Adv. Mater.* **2007**, *19*, 3589.
(14) Chandra, D.; Yang, S.; Lin, P. *Appl. Phys. Lett.* **2007**, *91*, 251912.
(15) Stafford, C. M.; Harrison, C.; Beers, K. L.; Karim, A.; Amis, E. J.; Vanlandingham, M. R.; Kim, H. C.; Volksen, W.; Miller, R. D.; Simonyi, E. E. *Nat. Mater.* **2004**, *3*, 545.
(16) Huang, J.; Juszkiewicz, M.; de Jeu, W. H.; Cerda, E.; Emrick, T.; Menon, N.; Russell, T. P. *Science* **2007**, *317*, 650.
(17) Denkov, N. D.; Velev, O. D.; Kralchevsky, P. A.; Ivanov, I. B.; Yoshimura, H.; Nagayama, K. *Nature* **1993**, *361*, 26.
(18) Jiang, P.; Bertone, J. F.; Hwang, K. S.; Colvin, V. L. *Chem. Mater.* **1999**, *11*, 2132.
(19) Prevo, B. G.; Kuncicky, D. M.; Velev, O. D. *Colloid. Surf. A* **2007**, *311*, 2.
(20) Xia, Y. N.; Whitesides, G. M. *Annu. Rev. Mater. Sci.* **1998**, *28*, 153.
(21) Zhang, Y.; Lo, C. W.; Taylor, J. A.; Yang, S. *Langmuir* **2006**, *22*, 8595.
(22) Lee, J. N.; Park, C.; Whitesides, G. M. *Anal. Chem.* **2003**, *75*, 6544.
(23) Guo, Q. J.; Teng, X. W.; Rahman, S.; Yang, H. *J. Am. Chem. Soc.* **2003**, *125*, 630.
(24) Santhanam, V.; Andres, R. P. *Nano Lett.* **2004**, *4*, 41.
(25) Kraus, T.; Malaquin, L.; Delamarche, E.; Schmid, H.; Spencer, N. D.; Wolf, H. *Adv. Mater.* **2005**, *17*, 2438.
(26) Kraus, T.; Malaquin, L.; Schmid, H.; Riess, W.; Spencer, N. D.; Wolf, H. *Nat. Nanotechnol.* **2007**, *2*, 570.
(27) Xia, Y. N.; Kim, E.; Zhao, X. M.; Rogers, J. A.; Prentiss, M.; Whitesides, G. M. *Science* **1996**, *273*, 347.
(28) Kim, S. O.; Solak, H. H.; Stoykovich, M. P.; Ferrier, N. J.; de Pablo, J. J.; Nealey, P. F. *Nature* **2003**, *424*, 411.
(29) Stoykovich, M. P.; Müller, M.; Kim, S. O.; Solak, H. H.; Edwards, E. W.; de Pablo, J. J.; Nealey, P. F. *Science* **2005**, *308*, 1442.
(30) Kosevich, A. M.; Lifshitz, E. M.; Landau, L. D.; Lifshitz, E. M., *Theory of Elasticity*, 3rd ed.; Butterworth-Heinemann: Woburn, MA, 1986; Vol. 7, p 195.
(31) Mullin, T.; Deschanel, S.; Bertoldi, K.; Boyce, M. C. *Phys. Rev. Lett.* **2007**, *99*, 084301.
(32) Lin, P.; Yang, S. *Appl. Phys. Lett.* **2007**, *90*, 241903.

NL0801531